Korean J. Chem. Eng., 35(2), 579-586 (2018)
DOI: 10.1007/s11814-017-0302-z

pISSN: 0256-1115
eISSN: 1975-7220

Simple modification with amine- and hydroxyl- group rich biopolymer on ordered mesoporous carbon/sulfur composite for lithium-sulfur batteries

Won-Gwang Lim*, Changshin Jo*,, Jinwoo Lee*,†, and Dong Soo Hwang**,***,†**

*Department of Chemical Engineering, Pohang University of Science & Technology, 77 Cheongam-ro, Nam-gu, Pohang, Gyeongbuk 37673, Korea
**School of Environmental Science and Engineering and Division of Interdisciplinary Bioscience and Bioengineering, Pohang University of Science & Technology, 77 Cheongam-ro, Nam-gu, Pohang, Gyeongbuk 37673, Korea
***Ocean Science and Technology Institute, Pohang University of Science and Technology, 77 Cheongam-ro, Nam-gu, Pohang, Gyeongbuk 37673, Korea
(*Received 21 August 2017 • accepted 25 October 2017*)

Abstract—Lithium-sulfur (Li-S) batteries are promising next generation batteries, and numerous porous carbons have been considered as the support materials for sulfur to address dissolution of poylsulfide. However, the weak binding energy of carbon with sulfur species causes poor cycle performance. We report that amine- and hydroxyl-rich biopolymer (chitosan) coated on ordered mesoporous carbon (OMC) can effectively capture soluble polysulfide. The strong binding of chitosan's amine- and hydroxyl-group with the polysulfides prevents dissolution of soluble intermediates and assists dispersion of insulating final products. In addition, as chitosan is insoluble in the electrolyte, chitosan coating on the cathode sustainably increases cycle stability and coulombic efficiency of Li-S batteries. Initial coulombic efficiency of chitosan modified OMC/S composite was 81.7% and specific capacities of chitosan modified OMC/S composite were 32.4% and 51.6% higher than those of bare OMC/S composite at 100th and 140th cycle, respectively.

Keywords: Lithium-sulfur Batteries, Mesoporous Carbon, Biopolymer Coating, Polysulfides, Improved Electrochemical Performance

INTRODUCTION

Lithium ion batteries (LIBs) are widely used due to their lightness, superior electrochemical stability, and cycle stability [1-4]. In general, LIBs use graphite as anode materials, and lithium transition metal oxides or phosphates as cathode materials [5-10]. Because the Li-ion insertion/extraction mechanism of these electrode materials is based on an intercalation reaction, LIBs have low energy density and therefore are not suitable for use in electric vehicles (EVs) and energy storage systems (ESSs), which require high energy density. Hence, to increase the energy density of the LIBs, another electrochemical system should be developed. Lithium-sulfur (Li-S) batteries are promising next-generation batteries because the reaction of sulfur (S_8+16Li→8Li_2S) in LIBs results in high theoretical capacity of 1,672 mA h g^{-1} and energy density of 2,600 W h kg^{-1} (commercial LIBs: ~380 W h kg^{-1}) [9,11]. Additionally, sulfur is abundant, inexpensive, and environmentally benign [12,13]. However, the commercialization of Li-S batteries still has a long way to go because the intrinsic electrical conductivity of elemental sulfur (~5×10^{-30} S cm^{-1} at room temperature) is low, soluble high order polysulfides (Li_2S_8-Li_2S_4) in the organic electrolytes gradually decrease the capacity of the Li-S batteries, and low order polysulfides (Li_2S_2/Li_2S) which are insulating and insoluble in the electrolytes, interrupt charge-transfer and disturb reversible oxidation due to their agglomeration on the cathode in Li-S batteries [14-17]. These problems eventually lead to poor cycle stability and low coulombic efficiency.

To address these problems, conductive support materials that can physically trap large amount of the insulating sulfur species are essential. As support materials for sulfur, previous research has considered substances such as porous carbons [18,19], highly ordered mesoporous carbon (OMC) [20-22], spherical hollow carbon [23, 24], bimodal porous carbon [25], and microporous carbon [26, 27]. However, extending the cycle life of Li-S batteries by using carbon support is still challenging due to weak binding between carbon and sulfur species. To overcome this limitation, the introduction of functional group on the surface of carbon has been proposed, and they improved cycling endurance of Li-S batteries due to strong affinity with sulfur species [28-34]. Especially, the amine group (-NH_2) has been used as a functional group to increase cycle stability of Li-S batteries. Park et al. reported aniline-modified OMC as a host material for Li-S batteries [28]. *Ab initio* calculations using density functional theory (DFT) proved that non-pair electrons in the amine group can interact strongly with sulfur species [28]. As a result, aniline-modified OMC showed improved capacity retention of 73% after 50 cycles compared with 51% retention in unmodified OMC. Coulombic efficiency was also increased to >98% from 92% after 50 cycles. Recently, Archer et al. reported that polyethylenimine (PEI) functionalized carbon nanotubes (CNT) could improve the cycle stability of Li-S batteries due to amine group in

†To whom correspondence should be addressed.
E-mail: dshwang@postech.ac.kr, jinwoo03@postech.ac.kr

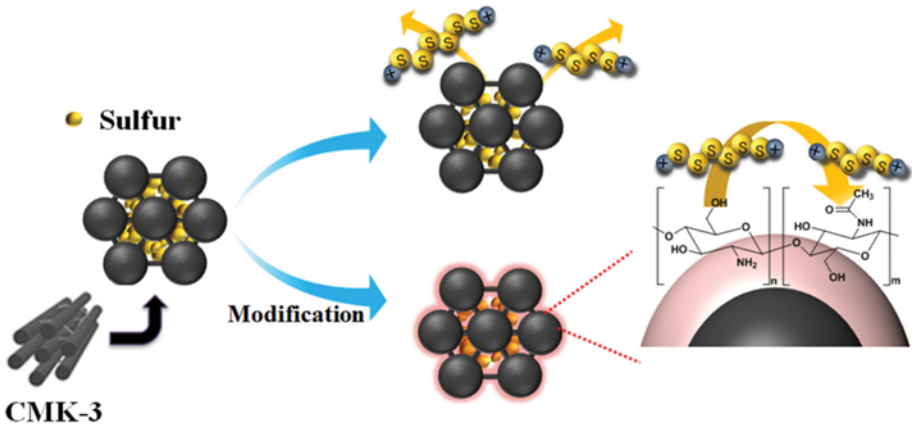

Fig. 1. Illustration of the effect of chitosan modification on ordered mesoporous carbon.

PEI [30]. The capacity retention of bare CNT was <50% after 100 cycles, PEI-modified CNT retained 79% of capacity even after 300 cycles. Although amine group on carbon surface extends the cycle life of the Li-S batteries, preparation of efficient host materials requires development of simple and inexpensive methods to modify the carbon by functionalizing it with amine group.

Recently, the use of functional biopolymers in LIB systems has been evaluated because the biopolymers are naturally abundant, inexpensive, and sustainable [35-37]. Beyond these advantages, biopolymers are easier to process than synthetic polymers such as polypyrrole, polyaniline, and poly (3,4-ethylenedioxythiophene), which are synthesized using toxic chemicals, in complicated synthesis processes, and require controlled experimental conditions [38-42]. Therefore, biopolymer-based surface modification can meet the requirements for simple, ecologically-benign synthesis.

In this work, we report a simple amine-functionalization on OMC (CMK-3)/sulfur composite using a chitosan biopolymer for cathode application in Li-S batteries (Fig. 1). The CMK-3 was impregnated with sulfur to make CMK3-S, which was then coated with chitosan that had been modified in a mild-acidic solution; the resulting chitosan coated CMK3-S (Chit-CMK3-S) was assessed as cathode in Li-S batteries. Chitosan, the second most abundant biopolymer, was selected as the modifying material because it has numerous amine- and hydroxyl-groups that provide binding motifs for polysulfides. In addition, electrostatic and van der Waals interactions can coat chitosan easily on the CMK-3/sulfur composite in dilute acidic condition [43,44], but the chitosan coated on CMK-3/sulfur composite is insoluble in organic electrolyte during charge/discharge of Li-S batteries. Therefore, chitosan can effectively link OMC to polysulfides. Because the amine group has been proven to be an effective functional group for Li-S batteries [28, 30], stable coating of chitosan on CMK-3/sulfur composite (Chit-CMK3-S) by simple method is expected to enhance the electrochemical properties of Li-S batteries. Due to strong affinity to sulfur species, amine groups effectively capture high order polysulfides (Li_2S_8-Li_2S_4), and assist distribution of insulating low order polysulfides (Li_2S_2/Li_2S). In addition, the hydrophilic nature of abundant hydroxyl groups on chitosan also can interact with sulfur species and disturb the dissolution of polysulfides [33,45]. Therefore, the combination of chitosan and OMC/S composite has improved the cycle stability and reversibility of Li-S batteries.

EXPERIMENTAL

1. Materials

Sulfur (99.998%, trace metals basis), carbon disulfide (CS_2, ≥99.9%), chitosan (medium molecular weight) and super-hydride solution (1.0 M lithium triethylborohydride in tetrahydrofuran) were purchased from Sigma-Aldrich. Acetic acid (99.7% purity) was purchased from Junsei Chemical Co., Ltd. All chemicals were used without further purification.

2. Synthesis of Chit-CMK3-S

Ordered mesoporous carbon, CMK-3 with pore size of 3 nm was prepared by a hard template method using SBA-15 silica, as described elsewhere [46]. Then, elemental sulfur was mixed into CMK-3 with CS_2. CS_2 was evaporated at room temperature (RT) after a few minutes. Heating the mixture of CMK-3 and sulfur to 155 °C under vacuum impregnated sulfur into CMK-3. To modify chitosan on CMK3-S composite, CMK3-S (0.1 g) was dispersed in deionized water (15 mL) and an extra 25 wt% of ethanol was added to improve the dispersion of CMK3-S. Chitosan solution was prepared by dissolving chitosan (0.8 g) in 3 wt% of acetic acid solution at RT. Then, CMK3-S solution was mixed with prepared chitosan solution and stirred at 40 °C for 12 h. The mixture was washed several times with deionized water to remove residual reactants and solvents, and to neutralize the pH. The resulting Chit-CMK3-S was dried at RT under vacuum.

3. Synthesis of Polysulfide Solution

Polysulfide was prepared as reported elsewhere [47]. Elemental sulfur was mixed with super-hydride solution in a suitable molecular ratio for 1 hour in an Ar-filled glove box to prepare Li_2S_4 as a representative of soluble polysulfide. Mixed solution was dried under vacuum, then washed with toluene several times; the resulting polysulfide was stored in Ar-filled glove box until use. For the polysulfide adsorption test, polysulfide solution was prepared by dispersing 4 mg polysulfide in 5 mL THF.

4. Material Characterization

The structures of CMK3-S and Chit-CMK3-S were analyzed

using scanning electron microscopy (S-4200 field emission SEM, Hitachi). Powder X-ray diffraction (XRD) patterns were obtained using a D/max-2500 diffractometer (Rigaku, Cu K_α radiation). Nitrogen adsorption and desorption analysis was conducted at 77 K using a Micromeritics TriStar II 3020 system. Surface area was calculated using the Brunauer-Emmett-Teller (BET), and pore size distribution was calculated using the Barrett-Joyner-Halenda (BJH) method based on the adsorption branch. Pores measured at relative pressure of 0.99. X-ray photoelectron spectroscopy (XPS) data were collected using VG Scientific Escalab 250 (Al K_α). Electron energy loss spectroscopy (EELS) mapping was performed using transmission electron microscopy (JEM-2200FS, field emission TEM, Jeol LTD). Thermogravimetric analysis (TGA, Perkin Elmer, USA) was used to calculate the amount of sulfur and chitosan that were loaded and modified on CMK-3 or CMK3-S. A polysulfide adsorption test was conducted using prepared polysulfide solution based on the BET surface area of each sample.

5. Electrochemical Characterization

Cathodes for Li-S batteries were prepared by mixing active materials (Chit-CMK3-S, or CMK3-S) with conducting carbon (Super P) and polyvinylidene fluoride (PVDF) binder in a weight ratio of 8 : 1 : 1 with N-methly-2-pyrrolidone (NMP). The resulting slurries were coated onto Al foil by doctor-blading, then dried at 60 °C for 12 h in an oven. The electrodes obtained were pressed and cut into round shapes. On average, 1.5-2.0 mg cm^{-2} of sulfur was loaded. A half-cell test was performed using coin-type cells (CR2032), which were fabricated in an Ar-filled glove box. The counter and reference electrodes were Li foil, the electrolyte was 1.0 M bis(trifluoromethane) sulfonamide lithium salt (LiTFSI) in mixed solvent of dimethoxymethane and 1,3-dioxolane (DME/DOL, 1 : 1 volume ratio, PANAX E-TEC Co., Korea) containing 2 wt% lithium nitrate ($LiNO_3$, 99.99%, metals basis, Sigma-Aldrich). The amount of electrolyte was fixed at 20 μL for 1 mg of sulfur. Considering that areal density of sulfur was 1.5-2.0 mg cm^{-2}, 30-40 μL of electrolyte was used for each coin-type cell. To measure electrochemical characteristics, WBCS-3000 battery cycler (WonATech Co., Korea) was used. To avoid irreversible reduction of $LiNO_3$ on the cathode surface at potentials <1.6 V (vs. Li/Li^+) [48], galvanostatic charge/discharge analysis was conducted in the potential range of 1.7 to 3.0 V at 0.2 C rate (1 C=1,672 mA g^{-1}). Electrochemical impedance spectroscopy (EIS) was conducted using a potentiostat (Reference 600, Gamry Instruments, USA), and recorded from 0.05 to 10^5 Hz at 5 mV magnitude. Coin-type cells were disassembled in an Ar-filled glove box and washed with dimethyl carbonate (DMC, 99.0%, Sigma-Aldrich) several times before EELS mapping. All specific capacity was calculated based on mass of sulfur; for fair comparison, each electrode material contained an identical amount of sulfur.

RESULT AND DISCUSSION

X-ray diffraction (XRD) patterns of the sulfur, CMK3-S and Chit-CMK3-S are shown in Fig. 2(a). The XRD pattern of sulfur matches the orthorhombic phase [49]. After impregnating sulfur into CMK-3, the sharp crystalline peak of sulfur in the XRD pattern vanished; it was also absent from the XRD pattern of Chit-CMK3-S. Only a broad peak at ~25° from amorphous carbon (CMK-3) remained; this observation indicates that sulfur was well impregnated into mesopores of CMK-3 [21], was well confined within them, and did not flow out of the pores in Chit-CMK3-S. The N_2 adsorption and desorption isotherms of each samples are shown in Fig. 2(b). As sulfur was partially impregnated into CMK-

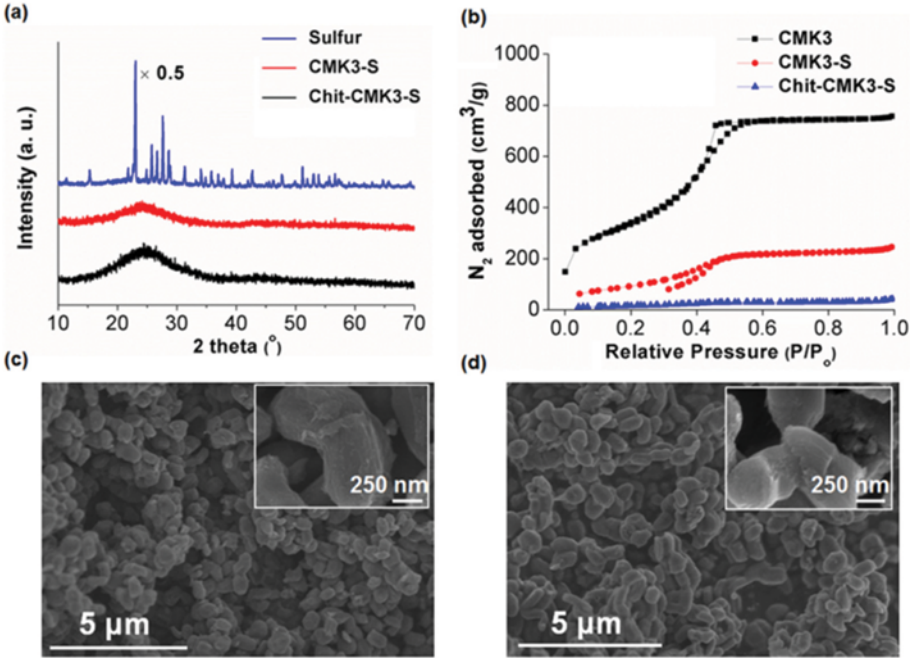

Fig. 2. (a) XRD patterns, (b) N_2 adsorption and desorption isotherm linear plot of CMK-3, CMK3-S, and Chit-CMK3-S. SEM images and higher magnified SEM images (inset) of (c) CMK3-S, (d) Chit-CMK3-S. Intensity of XRD peaks of sulfur was multiplied by 0.5 (×0.5).

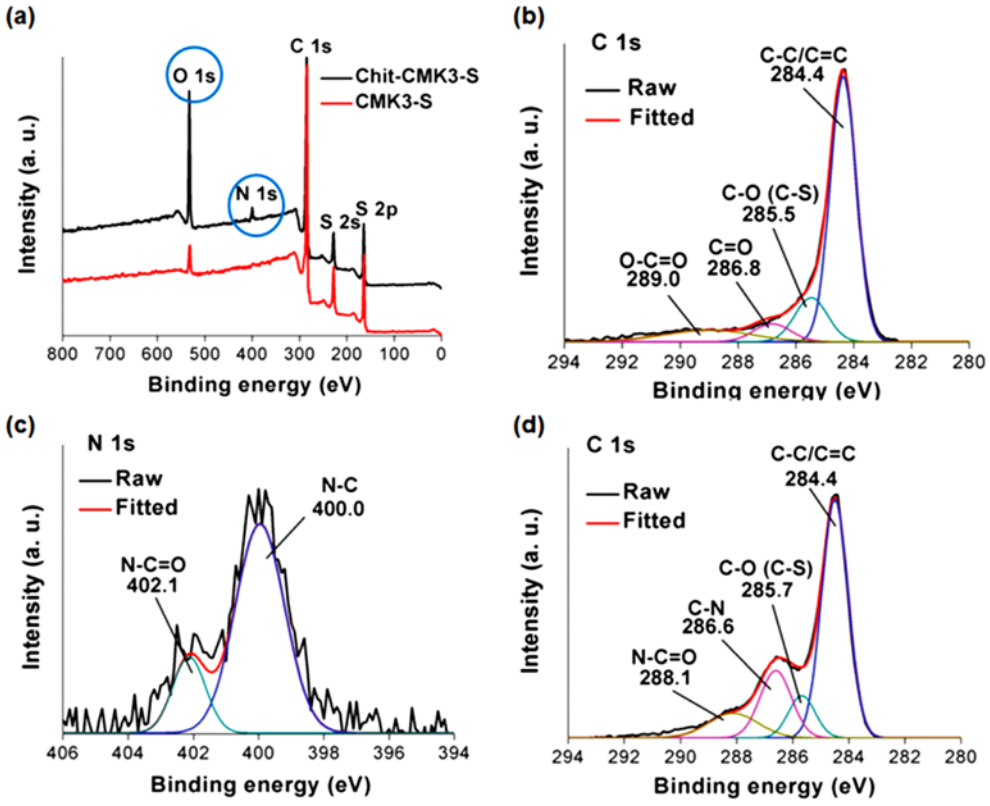

Fig. 3. XPS spectra of (a) wide scan survey, (b) C 1s region in CMK3-S, (c) N 1s region in Chit-CMK3-S, (d) C 1s region in Chit-CMK3-S.

3 and chitosan was modified on CMK3-S, BET surface area and pore volume decreased significantly from 1,233 $m^2 g^{-1}$ and 1.2 $cm^3 g^{-1}$ in bare CMK-3 to 346 $m^2 g^{-1}$ and 0.4 $cm^3 g^{-1}$ in CMK3-S, to 62 $m^2 g^{-1}$ and 0.07 $cm^3 g^{-1}$ in Chit-CMK3-S. Drastic reduction of surface area and pore volume means that mesopores of CMK-3 are filled with sulfur, and then coated by chitosan. Scanning electron microscopy (SEM) images of CMK3-S (Fig. 2(c)) and Chit-CMK3-S (Fig. 2(d)) show no noticeable non-porous particles (sulfur particles in 10-30 μm sizes in Fig. S1(a)); this result indicates that sulfur was confined inside the CMK-3, and it is consistent with XRD data (Fig. 2(a)). The Chit-CMK3-S did not show irregular aggregation of chitosan apart from CMK-3, and the innate morphology of CMK-3 (Fig. S1(b)) was maintained well in both CMK3-S and Chit-CMK3-S without any structural destruction (insets, Fig. 2(c), (d)).

X-ray photoelectron spectroscopy (XPS) was used to characterize the coated surface of chitosan on Chit-CMK3-S. As shown in Fig. 3(a), bare CMK3-S showed only the characteristic peaks of C 1s (285 eV), S 2s (228 eV), S 2p (164 eV), and O 1s (533 eV) [50, 51]. The O 1s peak corresponds to the carboxyl group and hydroxyl group of bare CMK-3. In contrast, the strong N 1s peak (amine group of chitosan) and strong O 1s peak (hydroxyl and ether groups of chitosan) support that chitosan was successfully modified on the CMK3-S surface. C 1s peaks of CMK3-S and Chit-CMK3-S were deconvoluted (Fig. 3(b), (d)). The C 1s deconvolution signals of CMK3-S show only C-O hydroxyl groups (285.5 eV) and O-C=O carboxyl group (289.1 eV), whereas those of Chit-CMK3-S show additional C-N amine bonds (286.6 eV) and N-C=O bonds (288.1 eV) [30,51]. The deconvoluted N 1s peak of Chit-CMK3-S (Fig. 3(c)) exhibits both N-C bonds (400.0 eV) and N-C=O bonds (402.1 eV), this result confirms that chitosan had coated the CMK3-S [50]. EELS mapping was also performed on electrode material

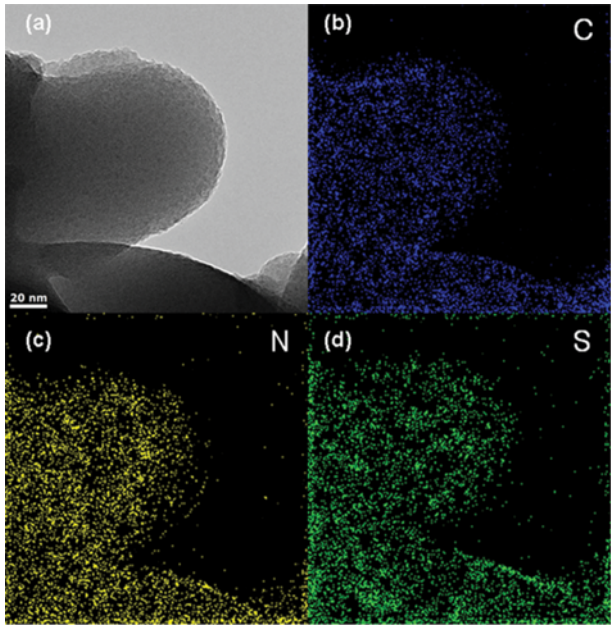

Fig. 4. (a) TEM image of Chit-CMK3-S. EELS mapping images of (b) carbon, (c) nitrogen, (d) sulfur in Chit-CMK3-S.

after the coin cell was disassembled at the 100th cycle (Fig. 4). As shown in Fig. 4(b)-(d), EELS mapping images of Chit-CMK3-S show that sulfur and nitrogen are well distributed inside the carbon matrix even after 100 cycles. The homogeneously-distributed nitrogen is mainly in the amine group of chitosan in Chit-CMK3-S. Thermogravimetric analysis (TGA) on the samples was also conducted to confirm the amount of sulfur and chitosan in Chit-CMK3-S (Fig. S2(a), (b)). The amount of sulfur in CMK3-S was 41%; for fair comparison, the amount of sulfur in Chit-CMK3-S was targeted to ~41% (characterized by elemental analysis). Thus, excluding 3.5% of decomposition of adsorbed water at <200 °C, weight loss of 46.1% in Chit-CMK3-S is contributed by both sulfur and chitosan (Fig. S2(b)). Considering that 28.3% of chitosan is decomposed to carbon under N_2 atmosphere (Fig. S2(c)), initial weight ratio of CMK-3 : sulfur : chitosan is 52 : 41 : 7 in Chit-CMK3-S.

To confirm the effect of chitosan modification on electrochemical performance of Li-S batteries, galvanostatic charge/discharge was performed at 0.2 C rate (1 C=1,672 mA g^{-1}) at RT. The voltage profiles of both CMK3-S (Fig. 5(a)) and Chit-CMK3-S (Fig. 5(b)) represent typical Li-S batteries. For instance, two plateaus occur during discharge. One plateau at ~2.3 V is mainly attributed to formation of high order polysulfides as intermediates during reduction of elemental sulfur (S_8). The second plateau at ~2.1 V is a result of electrochemical reduction of high order polysulfides to final products (Li_2S_2/Li_2S) [23]. During the charge process, only one plateau at 2.2-2.3 V occurs: it is due to electrochemical oxidation of polysulfides to sulfur (S_8). The peak at the beginning of charge process is due to energy barrier for activation of Li_2S [27]. During 140 cycles, the capacity of CMK3-S faded severely, but that of Chit-CMK3-S was retained well. Chit-CMK3-S also exhibits better cycle stability than CMK3-S (Fig. 5(c)). At the 100th cycle, specific capacity of CMK3-S was 658 mA h g^{-1} and faded severely to only 532 mA h g^{-1} at the 140th cycle. In contrast, the specific capacity of Chit-CMK3-S was 871 mA h g^{-1} (~32.4% higher than that of CMK3-S), at the 100th cycle, and 807 mA h g^{-1} (~51.6% higher than that of CMK3-S) at the 140th cycle. Up to the 140th cycle, the capacity faded by 0.36% per cycle in CMK3-S, but by 0.20%, per cycle in Chit-CMK3-S. Although OMC can mitigate dissolution of high order polysulfides into electrolyte, simple physical confinement of polysulfides into the pore of OMC is insufficient to prevent the shuttle effect. Dissolution of high order polysulfides into electrolyte during charge and discharge process causes loss of sulfur and accelerates capacity fading. The increase in cycling stability in Chit-CMK3-S was achieved because amine- and hydroxyl-groups in chitosan have strong affinity for sulfur species, and therefore effectively capture high order polysulfides and prevent dissolution of soluble intermediates, and thereby increase number of cycles over which sulfur can be utilized. Strong binding of chitosan with polysulfides is demonstrated in Fig. S3. To compare the binding strength of polysulfides to carbon and chitosan, a polysulfide adsorption test was conducted with identical surface area of each sample. After mixing each solution with prepared polysulfides, chitosan solution is more transparent than CMK-3 solution, presumably due to stronger binding of polysulfides to amine- and hydroxyl-groups in chitosan compared with the chitosan-free carbon support (Fig. S3(a)). The adsorption test result of CMK3-S and Chit-CMK3-S also supports stronger affinity of chitosan with polysulfides (Fig. S3(b)). The differential capacity (dQ/dV) plot

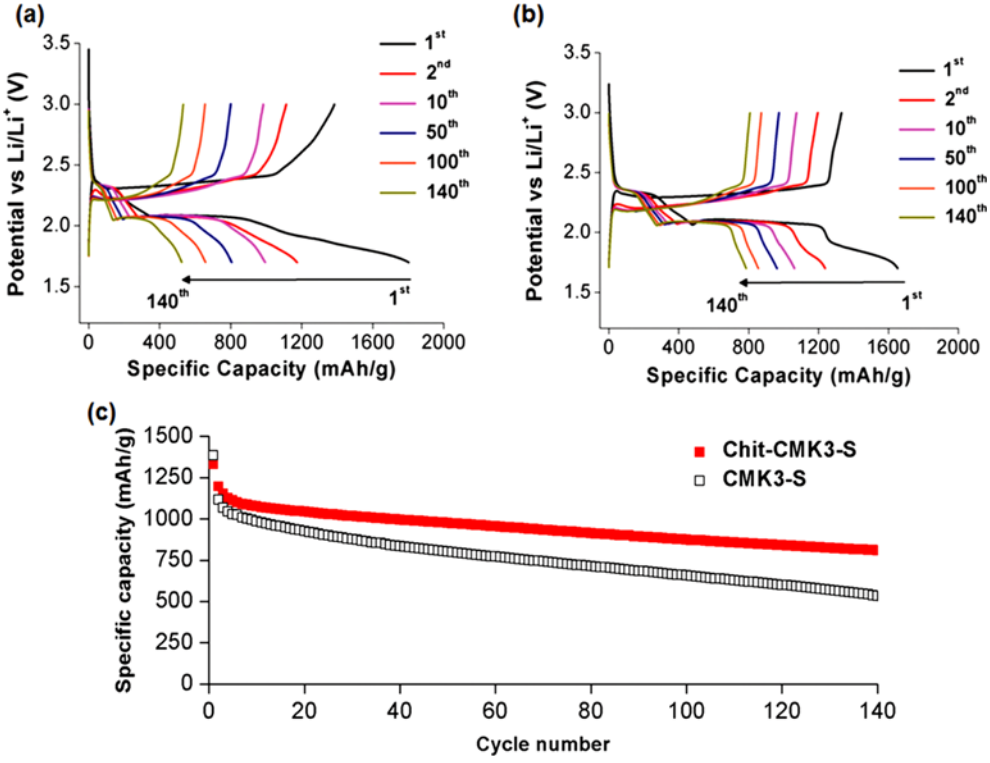

Fig. 5. Voltage profiles of (a) CMK3-S and (b) Chit-CMK3-S. (c) Galvanostatic charge/discharge profile at 0.2 C rate (1 C: 1,672 mA g^{-1}).

(Fig. S4) is consistent with the voltage profile, in showing cathodic peaks at ~2.3 V and ~2.1 V that correspond to the high, and low voltage plateau, respectively. The intensities of the cathodic peaks decreased drastically in CMK3-S, but Chit-CMK3-S maintained its redox reaction well. It also supports the improved electrochemical performance by chitosan modification on CMK3-S composite. To study the reversibility of cathode for Li-S batteries, coulombic efficiencies (CEs) were calculated (Fig. 6(a)). Initial coulombic efficiency of Chit-CMK3-S was 81.7%, but 76.8% in bare CMK3-S and Chit-CMK3-S had higher CE than did CMK3-S over 100 cycles. Despite high coulombic efficiency in both Chit-CMK3-S and CMK3-S due to the $LiNO_3$ additive in electrolyte, higher CE of Chit-CMK3-S than that of CMK3-S indicates the improved reversibility of cathode by chitosan coating. To further prove the effect of chitosan modification on OMC/S composite, the capacity of higher voltage plateau (Fig. 6(b)) was calculated before the beginning of the lower voltage plateau at 2.1 V but including the sloping region and higher voltage plateau mainly from formation of high order polysulfides. Retention of capacity contributed by high order polysulfides is higher in Chit-CMK3-S than in bare CMK3-S. This difference means that soluble high order polysulfides produced at near 2.3 V are easily dissolved in electrolyte without chitosan, so the dissolved sulfur can no longer participate in redox reactions. Specific capacity of the lower voltage plateau (Fig. 6(c)) was calculated only from voltage <2.1 V, at which low order polysulfides form. Specific capacity of the lower voltage plateau in CMK3-S declined rapidly, to 65% at the 100th cycle and to 50% at the 140th cycle. However, the capacity of Chit-CMK3-S was 80% at the 100th cycle and 75% even at the 140th cycle. Decline of capacity in the lower voltage plateau is attributed to two factors: (1) Loss of high order polysulfides at higher voltage plateau (near 2.3 V), prevented further reduction to low order polysulfides. Moreover, capacity fading is more severe in lower voltage plateau than in the higher voltage plateau (Fig. 6(b), (c)). This difference implies that capacity fading in the lower voltage plateau is also affected by (2) lack of participation of low order polysulfides during redox reactions. Low order polysulfides are insulants and tend to aggregate with each other [28]. The aggregated insulants hamper charge-transfer; to avoid reduction of capacity, these low order polysulfides must be dispersed throughout the conductive support. Based on reason (2), the amine group of chitosan may interact with low order polysulfides and improve their dispersion. Eventually, this interaction enables final products (Li_2S_2/Li_2S) to participate in further redox reaction. Electrochemical impedance spectroscopy (EIS) analysis was performed to study internal resistance of each electrochemical system. Nyquist plots were collected from EIS analysis of both samples (Fig. 7(a), (b)) before and after 140 cycles. Each Nyquist plot consists of two semicircles in high-to-medium frequency region, and sloped line in the low frequency region. Generally, while the semicircle shown in high frequency region is related to layers deposited on the surface of cathode, the semicircle in medium frequency region is related to charge-transfer resistance, and the sloping line is related to resistance of Warburg diffusion [52]. In Nyquist plots of CMK3-S and Chit-CMK3-S before galvanostatic charge and discharge (Fig. 7(a)), Chit-CMK3-S had a larger semi-circle than did bare CMK3-S due to the low electrical conductivity of chitosan coated on the surface of the cathode. However, after 140 cycles, the semi-circle size of Chit-CMK3-S shown in high frequency region decreased significantly and smaller than that of CMK3-S (Fig. 7(b)). It indicates that the dense insulating layer of low order polysulfides (Li_2S_2/Li_2S) is prevented to be deposited on the surface of the cathode in Chit-CMK3-S. Considering that amine group can interact effectively with low order polysulfides, the amine group in chitosan may lead

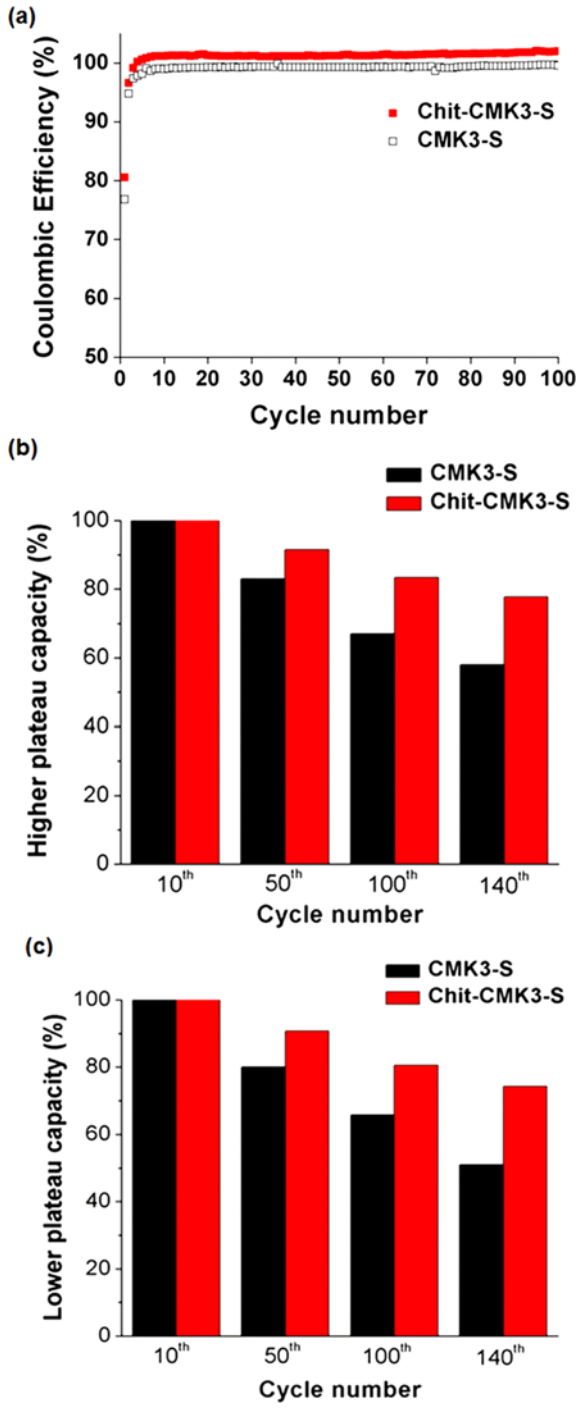

Fig. 6. (a) Coulombic efficiency of CMK3-S and Chit-CMK3-S. Normalized capacity profiles of (b) higher voltage plateau and (c) lower voltage plateau of CMK3-S and Chit-CMK3-S.

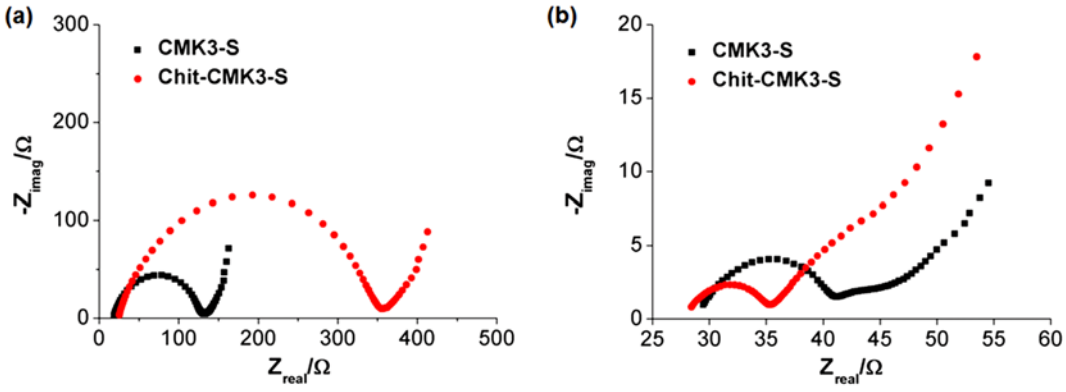

Fig. 7. Nyquist plots of CMK3-S and Chit-CMK3-S (a) before charge/discharge process, (b) after 140 cycles.

to well-distributed formation of insulating products, compared with those of CMK3-S electrode. Improved delocalization of insulating low order polysulfides assists significant decrease of the semicircle size in Chit-CMK3-S. In contrast to Chit-CMK3-S, low order polysulfides in CMK3-S form irregular aggregates that increase charge-transfer resistance. Improved charge-transfer of Chit-CMK3-S is also demonstrated by comparing energy barrier with bare CMK3-S (Fig. S4(c)). At the beginning of charging, an energy barrier is usually observable in Li-S batteries because additional energy is required to activate insulating Li_2S. At the 50^{th} cycle, the energy barrier was smaller in Chit-CMK3-S that in CMK3-S. Considering that the height of the energy barrier usually depends on conductivity or charge-transfer resistance, amine group in chitosan may help the dispersion of insulating materials (Li_2S_2/Li_2S), and thereby decrease the charge-transfer resistance; this hypothesis is consistent with EIS results.

CONCLUSION

We have reported a simple and stable chitosan coating on a composite of ordered mesoporous carbon and sulfur, to improve the electrochemical performance of Li-S batteries. Chitosan, with abundant amine and hydroxyl moieties, showed strong affinity with polysulfides. Therefore, chitosan coating on the OMC/sulfur composite mitigated polysulfides dissolution into the electrolyte, and consequently the loss of active materials from the cathode was reduced. Additionally, the amine group in chitosan also improved the dispersion of insulating low order polysulfides and decreased the charge-transfer resistance after numerous cycles. Eventually, the chitosan-modified cathode improved the cycle stability and CE of Li-S batteries.

ACKNOWLEDGEMENTS

The authors gratefully acknowledge the support by Basic Research Laboratory program and the National Research Foundation of Korea Grant funded by the Korean Government (NRF-2016R1A4A1010735 and NRF-2016M3D3A1A01913258), and the Marine Biotechnology program (Marine BioMaterials Research Center) funded by the Ministry of Oceans and Fisheries, Korea (D11013214H480000110). This work was also supported by the Korea Institute of Energy Technology Evaluation and Planning (KETEP) and Ministry of Trade, Industry & Energy (MOTIE) of the Republic of Korea (No. 201741030201600).

SUPPORTING INFORMATION

Additional information as noted in the text. This information is available via the Internet at http://www.springer.com/chemistry/journal/11814.

REFERENCES

1. A. S. Arico, P. Bruce, B. Scrosati, J.-M. Tarascon and W. Van Schalkwijk, *Nat. Mater.*, **4**, 366 (2005).
2. H. Park, D. H. Yeom, J. Kim and J. K. Lee, *Korean J. Chem. Eng.*, **32**, 178 (2015).
3. J.-M. Tarascon and M. Armand, *Nature*, **414**, 359 (2001).
4. N. Venugopal, W.-S. Kim and T. Yu, *Korean J. Chem. Eng.*, **33**, 1500 (2016).
5. A. R. Armstrong and P. G. Bruce, *Nature*, **381**, 499 (1996).
6. J. Cho, Y. J. Kim and B. Park, *Chem. Mater.*, **12**, 3788 (2000).
7. F. Jiao, K. M. Shaju and P. G. Bruce, *Angew. Chem. Int. Ed.*, **44**, 6550 (2005).
8. K.-M. Kang, H.-W. Kim and H.-Y. Kwak, *Korean J. Chem. Eng.*, **33**, 688 (2016).
9. K. Mizushima, P. Jones, P. Wiseman and J. Goodenough, *Mater. Res. Bull.*, **15**, 783 (1980).
10. D.-L. Vu and J.-w. Lee, *Korean J. Chem. Eng.*, **33**, 514 (2016).
11. G. Xu, B. Ding, J. Pan, P. Nie, L. Shen and X. Zhang, *J. Mater. Chem. A*, **2**, 12662 (2014).
12. P. G. Bruce, S. A. Freunberger, L. J. Hardwick and J.-M. Tarascon, *Nat. Mater.*, **11**, 19 (2012).
13. S.-H. Yeon, W. Ahn, K.-H. Shin, C.-S. Jin, K.-N. Jung, J.-D. Jeon, S. Lim and Y. Kim, *Korean J. Chem. Eng.*, **32**, 867 (2015).
14. A. F. Hofmann, D. N. Fronczek and W. G. Bessler, *J. Power Sources*, **259**, 300 (2014).
15. X. Ji and L. F. Nazar, *J. Mater. Chem.*, **20**, 9821 (2010).
16. A. Manthiram, Y. Fu and Y.-S. Su, *Acc. Chem. Res.*, **46**, 1125 (2012).
17. Y. X. Yin, S. Xin, Y. G. Guo and L. J. Wan, *Angew. Chem. Int. Ed.*,

52, 13186 (2013).
18. J. Lee, J. Kim and T. Hyeon, *Adv. Mater.*, **18**, 2073 (2006).
19. Y. Ye, C. Jo, I. Jeong and J. Lee, *Nanoscale*, **5**, 4584 (2013).
20. X. Ji, K. T. Lee and L. F. Nazar, *Nat. Mater.*, **8**, 500 (2009).
21. X. Li, Y. Cao, W. Qi, L. V. Saraf, J. Xiao, Z. Nie, J. Mietek, J.-G. Zhang, B. Schwenzer and J. Liu, *J. Mater. Chem.*, **21**, 16603 (2011).
22. J. r. G. Werner, S. S. Johnson, V. Vijay and U. Wiesner, *Chem. Mater.*, **27**, 3349 (2015).
23. N. Jayaprakash, J. Shen, S. S. Moganty, A. Corona and L. A. Archer, *Angew. Chem.*, **123**, 6026 (2011).
24. W. Zhou, X. Xiao, M. Cai and L. Yang, *Nano Lett.*, **14**, 5250 (2014).
25. G. He, X. Ji and L. Nazar, *Energy Environ. Sci.*, **4**, 2878 (2011).
26. S. Xin, L. Gu, N.-H. Zhao, Y.-X. Yin, L.-J. Zhou, Y.-G. Guo and L.-J. Wan, *J. Am. Chem. Soc.*, **134**, 18510 (2012).
27. Y. Yang, G. Zheng, S. Misra, J. Nelson, M. F. Toney and Y. Cui, *J. Am. Chem. Soc.*, **134**, 15387 (2012).
28. J. H. Kim, T. Kim, Y. C. Jeong, K. Lee, K. T. Park, S. J. Yang and C. R. Park, *Adv. Energy Mater.*, **5**, 1500268 (2015).
29. G. C. Li, G. R. Li, S. H. Ye and X. P. Gao, *Adv. Energy Mater.*, **2**, 1238 (2012).
30. L. Ma, H. L. Zhuang, S. Wei, K. E. Hendrickson, M. S. Kim, G. Cohn, R. G. Hennig and L. A. Archer, *ACS Nano*, **10**, 1050 (2015).
31. Y. Yang, G. Yu, J. J. Cha, H. Wu, M. Vosgueritchian, Y. Yao, Z. Bao and Y. Cui, *ACS Nano*, **5**, 9187 (2011).
32. G. Zheng, Q. Zhang, J. J. Cha, Y. Yang, W. Li, Z. W. Seh and Y. Cui, *Nano Lett.*, **13**, 1265 (2013).
33. G. Zhou, L.-C. Yin, D.-W. Wang, L. Li, S. Pei, I. R. Gentle, F. Li and H.-M. Cheng, *ACS Nano*, **7**, 5367 (2013).
34. C. Zu and A. Manthiram, *Adv. Energy Mater.*, **3**, 1008 (2013).
35. E. Khor and L. Y. Lim, *Biomaterials*, **24**, 2339 (2003).
36. D. Klemm, B. Heublein, H. P. Fink and A. Bohn, *Angew. Chem. Int. Ed.*, **44**, 3358 (2005).
37. E. Raymundo-Piñero, F. Leroux and F. Béguin, *Adv. Mater.*, **18**, 1877 (2006).
38. J. Fanous, M. Wegner, J. Grimminger, A. n. Andresen and M. R. Buchmeiser, *Chem. Mater.*, **23**, 5024 (2011).
39. Y. Fu and A. Manthiram, *Chem. Mater.*, **24**, 3081 (2012).
40. L. Wang, X. He, J. Li, J. Gao, J. Guo, C. Jiang and C. Wan, *J. Mater. Chem.*, **22**, 22077 (2012).
41. F. Wu, J. Chen, L. Li, T. Zhao and R. Chen, *J. Phys. Chem. C*, **115**, 24411 (2011).
42. W. Zhou, Y. Yu, H. Chen, F. J. DiSalvo and H. c. D. Abruña, *J. Am. Chem. Soc.*, **135**, 16736 (2013).
43. D. W. Lee, C. Lim, J. N. Israelachvili and D. S. Hwang, *Langmuir*, **29**, 14222 (2013).
44. C. Lim, D. W. Lee, J. N. Israelachvili, Y. Jho and D. S. Hwang, *Carbohydr. Polym.*, **117**, 887 (2015).
45. C. Zu and A. Manthiram, *Adv. Energy Mater.*, **3**, 1008 (2013).
46. S. Jun, S. H. Joo, R. Ryoo, M. Kruk, M. Jaroniec, Z. Liu, T. Ohsuna and O. Terasaki, *J. Am. Chem. Soc.*, **122**, 10712 (2000).
47. X. Liang, C. Hart, Q. Pang, A. Garsuch, T. Weiss and L. F. Nazar, *Nat. Commun.*, **6**, 5682 (2015).
48. S. S. Zhang, *Electrochim. Acta*, **70**, 344 (2012).
49. C. Wang, W. Wan, J.-T. Chen, H.-H. Zhou, X.-X. Zhang, L.-X. Yuan and Y.-H. Huang, *J. Mater. Chem. A*, **1**, 1716 (2013).
50. H. J. Kim, I.-S. Bae, S.-J. Cho, J.-H. Boo, B.-C. Lee, J. Heo, I. Chung and B. Hong, *Nanoscale Res. Lett.*, **7**, 1 (2012).
51. Q. Pang, J. Tang, H. Huang, X. Liang, C. Hart, K. C. Tam and L. F. Nazar, *Adv. Mater.*, **27**, 6021 (2015).
52. Y. Fu, Y.-S. Su and A. Manthiram, *ACS Appl. Mater. Interfaces*, **4**, 6046 (2012).

Supporting Information

Simple modification with amine- and hydroxyl- group rich biopolymer on ordered mesoporous carbon/sulfur composite for lithium-sulfur batteries

Won-Gwang Lim*, Changshin Jo*,, Jinwoo Lee*,†, and Dong Soo Hwang**,***,†**

*Department of Chemical Engineering, Pohang University of Science & Technology,
77 Cheongam-ro, Nam-gu, Pohang, Gyeongbuk 37673, Korea
**School of Environmental Science and Engineering and Division of Interdisciplinary Bioscience and Bioengineering,
Pohang University of Science & Technology, 77 Cheongam-ro, Nam-gu, Pohang, Gyeongbuk 37673, Korea
***Ocean Science and Technology Institute, Pohang University of Science and Technology,
77 Cheongam-ro, Nam-gu, Pohang, Gyeongbuk 37673, Korea
(*Received 21 August 2017 • accepted 25 October 2017*)

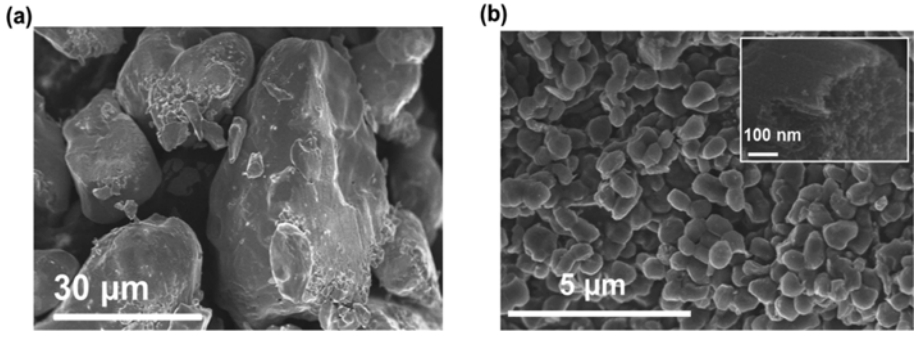

Fig. S1. SEM images of (a) elemental sulfur and (b) bare CMK-3.

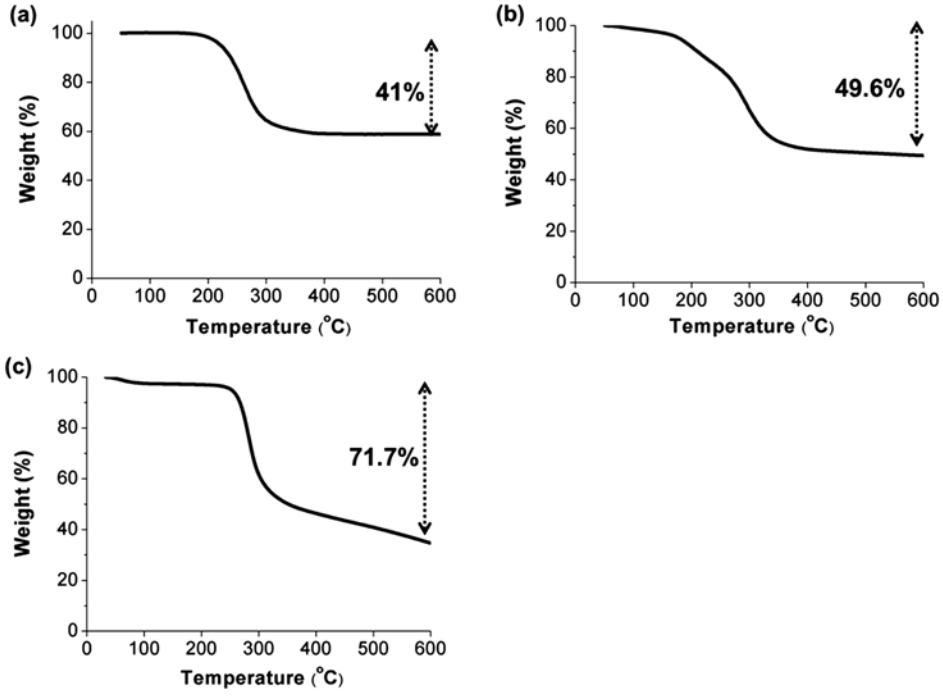

Fig. S2. TGA data of (a) CMK3-S, (b) Chit-CMK3-S, and (c) chitosan. All of TGA data were measured under nitrogen atmosphere with 5 °C/min rate.

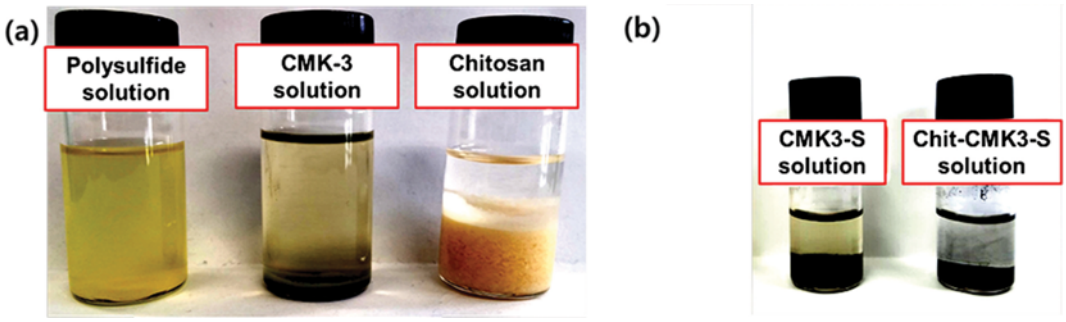

Fig. S3. Polysulfide adsorption test of (a) bare CMK-3 and chitosan without sulfur impregnation, (b) CMK3-S and Chit-CMK3-S.

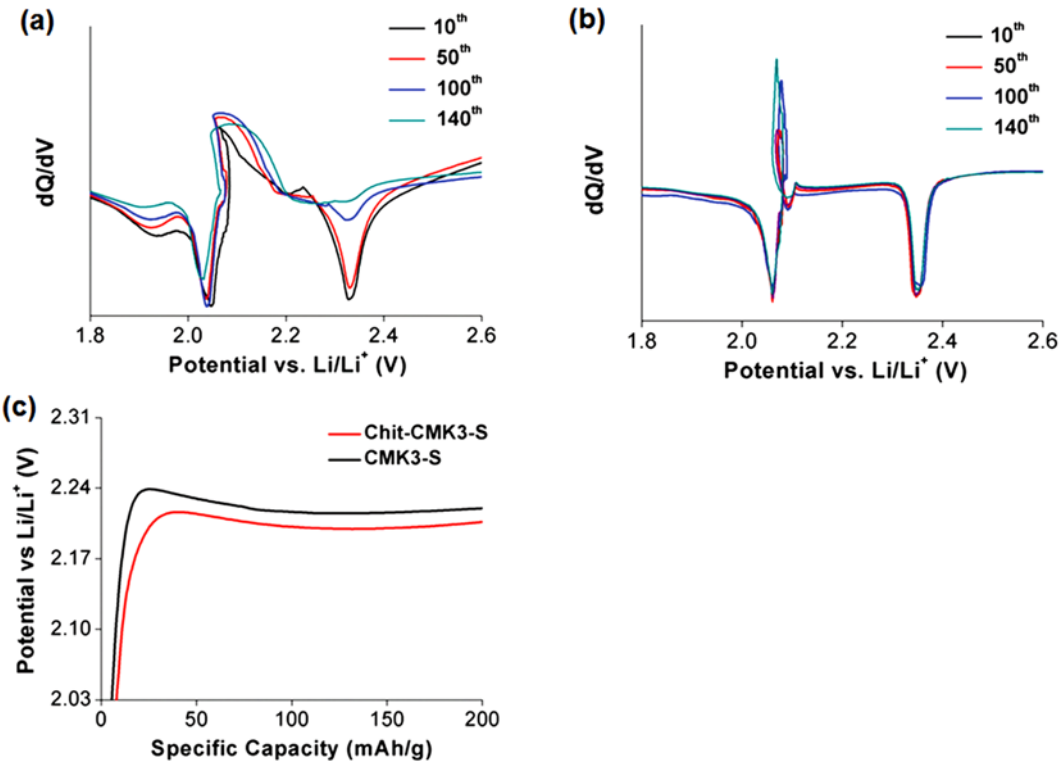

Fig. S4. Differential capacity (dQ/dV) plot of (a) CMK3-S and (b) Chit-CMK3-S. (c) Magnified voltage profile of CMK3-S and Chit-CMK3-S at the beginning of charge. Differential capacity plot is calculated from galvanostatic charge and discharge profile.